

Thesis, University of Manitoba (1983).

9. P.W.F. Alons, E.R. Siciliano and M.J. Leitch, Technical Progress Report 1985, University of Colorado, NPL 1004, p. 2; and P.W.F. Alons, private communication.
10. N. Willis, L. Bimbot, N. Koori, Y. Le Bornec, F. Reide, A. Willis and C. Wilkin, J. Phys. G: Nucl. Phys. **7** (1981) L195.
11. W.R. Falk et al., TRIUMF Experiment No. 413.
12. G.M. Huber, G.J. Lolos, R.D. Bent, K.H. Hicks, P.W. Walden, S. Yen, X. Aslanoglou, E.G. Auld and W.R. Falk, Phys. Rev. **C37** (1988) 1161.
13. G.M. Huber, G.J. Lolos, E.L. Mathie, Z. Papandreou, K.H. Hicks, P.L. Walden, S. Yen, X. Aslanoglou, E.G. Auld and W.R. Falk, Phys. Rev. **C 36** (1987) 1058.
14. J.M. Eisenberg and D.S. Koltun, Theory of Meson Interactions with Nuclei, (John Wiley and Sons, New York, 1980), p. 117.
15. J.V. Noble, Nucl. Phys. **A244** (1975) 526.
16. H.J. Weber and J.M. Eisenberg, Nucl. Phys. **A312** (1978) 201.
17. S.K. Young and W.R. Gibbs, Phys. Rev. **C17** (1978) 837.

## $^{12}\text{C}(p,\pi^+n)$ COINCIDENCE MEASUREMENT

E. Korkmaz\*, S.E. Vigdor, W.W. Jacobs, S.M. Aziz, L.C. Bland, H. Nann,  
*Indiana University Cyclotron Facility, Bloomington, Indiana 47405*

and J.D. Brown

*Department of Physics, Princeton University, Princeton, New Jersey 08554*

A current focus of the IUCF pion production program is on studying the extent to which  $A(p,\pi^\pm)$  reactions can be viewed as resulting from quasifree  $NN \rightarrow NN\pi$  processes in the nucleus.<sup>1,2</sup> Evidence in favor of a quasifree mechanism is particularly striking for  $A(\bar{p},\pi^+)A+1$  reactions, where analyzing power angular distributions  $[A_y(\theta)]$  for continuum production, and for nearly all strong transitions to discrete residual states as well, are similar to results for  $\bar{p}p \rightarrow d\pi^+$ , when the latter are transformed to the nucleon-nucleus reference frame.<sup>1</sup> These  $A_y(\theta)$  are large and negative over most of the angle range. In  $(\bar{p},\pi^+)$  measurements for several lp-shell target nuclei,<sup>1,3</sup> however, we have observed typically one, sometimes two, strong anomalous transitions – to relatively sharp states at high excitation ( $E_x \sim 14\text{-}23$  MeV) – with  $A_y \simeq 0$  at all angles. It is important to understand the nature of the anomalous final states, since these transitions may provide a clue essential to a more complete understanding of pion production from nuclei.

One plausible explanation<sup>1</sup> concerning the anomalous states observed in  $^{12}\text{C}$ ,  $^{13}\text{C}(\bar{p},\pi^+)$  at 21.4 MeV in  $^{13}\text{C}$  and 23.2 MeV in  $^{14}\text{C}$  is that they are isospin-mixed. A  $(p,\pi^+)$  transition to a  $T_>$  state in the final nucleus would involve a  $\Delta T=3/2$  amplitude, which is known<sup>1</sup> from  $(p,\pi^-)$  studies to be characterized by  $A_y$  of opposite sign and of smaller magnitude than is typical for  $\Delta T=1/2$  transitions. A suitable  $T_> - T_<$  admixture could conceivably account for the observed analyzing powers, cross section magnitudes, and

widths of the anomalous final states. Furthermore, the anomalous transition in  $^{12}\text{C}(p,\pi^+)$  is to a  $^{13}\text{C}$  state at  $E_x=21.4$  MeV, where previous  $^{13}\text{C}(\pi^\pm,\pi^\pm')$  results have suggested the existence of  $7/2^+$  or  $9/2^+$  states with possible isospin mixing as well. [An alternative interpretation<sup>1</sup> would be to view these states as  $T_<$  states with very high spin (e.g.,  $7^+$  in  $^{14}\text{C}$  and  $13/2^-$  in  $^{13}\text{C}$ ). The results<sup>5</sup> of recently completed studies of the  $^{11}\text{B}(\alpha,p)^{14}\text{C}$  and  $^{11}\text{B}(\alpha,d)^{13}\text{C}$  reactions – carried out mainly to test this  $T_<$  interpretation – do not support such an interpretation for the  $^{13}\text{C}$  state.]

We have initiated a  $^{12}\text{C}(p,\pi^+n)$  experiment in order to investigate the isospin nature of this  $^{13}\text{C}$  excited state. The aim was to look for evidence of the sequential neutron decay of the 21.4-MeV state by measuring  $^{12}\text{C}(p,\pi^+n)$  coincidence yields. If the state corresponds to an M4 excitation from the  $^{13}\text{C}_{g.s.}$ , as suggested by  $(\pi,\pi')$  and  $(e,e')$  results, then it might well have a significant branching ratio for neutron decay. For example, if the state were predominantly a  $7/2^+$ ,  $T=3/2$  state, one would then expect a dominant decay branch (via  $d_{5/2}$  neutron emission) to the  $1^+$ ,  $T=1$  (15.11 MeV) state in  $^{12}\text{C}$ , while a  $T=1/2$  state of similar configuration would decay preferentially to the  $1^+$ ,  $T=0$  (12.71 MeV) or  $2^+$ ,  $T=0$  (4.44 MeV) states. An isospin-mixed parent state might have significant decay branches to both  $T=0$  and  $T=1$   $^{12}\text{C}$  states. If  $J^\pi = 9/2^+$  for the 21.4-MeV state, then one should see decay neutrons leading to the 4.44-MeV state from a  $T=1/2$  parent component, and to the 16.1-MeV,  $2^+$ ,  $T=1$  state from a  $T=3/2$  parent component. In the case of an isospin-mixed parent state, one could conceivably get any value for the relative branching ratio ( $\Gamma_r$ ) for decay to  $T=0$  vs  $T=1$  daughter states, depending on the relative amplitudes and phases of the initial  $T=1/2$  and  $T=3/2$  components. The fact remains, however, that observation of a large (small) value for  $\Gamma_r$  would indicate a predominant  $T=1/2$  ( $T=3/2$ ) parent state. If the 21.4-MeV state had  $J^\pi$  different from  $7/2^+$  or  $9/2^+$ , then the  $(p,\pi^+n)$  coincidence spectrum would still be desirable, as other n-decay channels might be detected.

Such a coincidence measurement is very difficult given the small absolute  $(p,\pi^+)$  near-threshold cross section ( $\sim$  a few hundred nb/sr for the strongest transitions), even with the large solid angle and excellent particle identification of the QQSP magnetic spectrometer for the pions. The real-to-accidental ratio should be enhanced for the events of interest, because we are searching for coincidences between relatively sharp peaks in both the pion and neutron spectra.

The  $^{12}\text{C}(p,\pi^+n)$  measurement was carried out at IUCF using an unpolarized proton beam of energy 200 MeV. The beam intensity was limited to  $\sim 10$  nA in order to diminish the accidental-to-real coincidence ratio, while maintaining a reasonable real coincidence count rate. The  $^{12}\text{C}$  target thickness was  $54.5$  mg/cm<sup>2</sup>. The pions were detected at  $\theta_{lab}^\pi = 30^\circ$  to the right of the beam using the IUCF QQSP pion spectrometer<sup>6</sup>. The neutrons were detected with 7 neutron counters positioned in the reaction plane on the left-hand side of the beam line. The distance between the target and the center of each counter was 217 cm. The angle range covered by the neutron detectors was  $23^\circ \leq \theta_{lab}^n \leq 48^\circ$ . Each n-counter was a NE213 liquid scintillator, enclosed in a cylindrical glass container of 5" depth. Two of the detectors were commercial ones already in use in the lab; we built the remaining five. A thin plastic scintillator (1/8" thick) was placed in front of each counter and used to veto charged-particle events. (See Fig. 1).

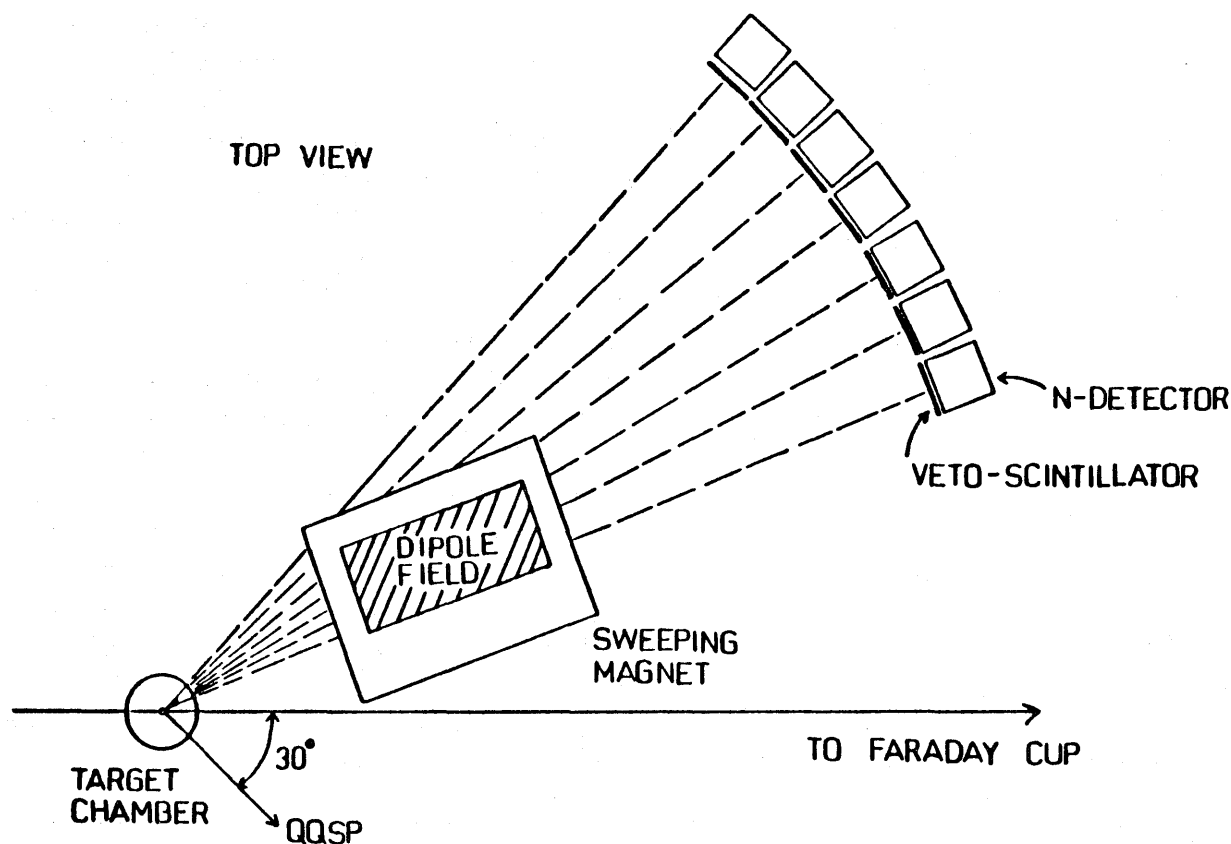
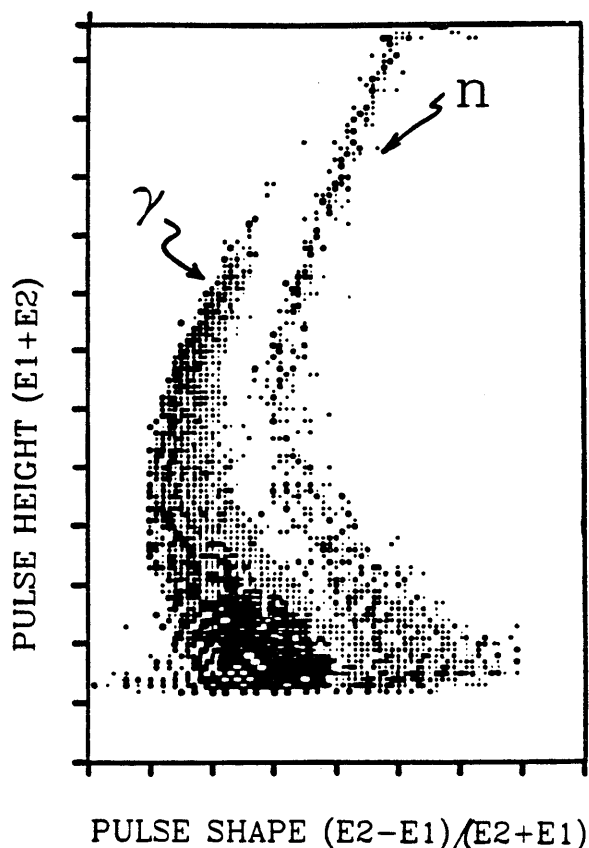


Figure 1. Experimental setup for the  $^{12}\text{C}(p,\pi^+n)$  measurement. The neutron detectors cover the angle range  $23^\circ \leq \theta_{lab}(n) \leq 48^\circ$ . The sweeping magnet deflects the high-energy elastically or inelastically scattered protons towards more forward angles.

Two test runs, taken prior to the production run, indicated the need for reducing the large singles count rates in the liquid scintillator detectors, arising mainly from elastically or inelastically scattered protons. These large count rates introduced serious phototube gain instabilities as well as other undesirable experimental features. This problem was cured, to a large extent, by the installation of a C-shaped sweeping magnet (dipole) in between the target chamber and the detectors, to deflect the high-energy protons toward smaller angles. These test runs also revealed that high-resolution pulse-shape discrimination (PSD) between low-energy neutron and photon events was critical for the measurement, because the singles rate of room background photons (uncorrelated with the cyclotron RF signal) in the time range of interest for the low-energy neutrons was about an order of magnitude larger than the neutron rate. The quality of PSD was affected, among other things, by the very low detector threshold required and by the large dynamic range of the scintillator electronics. Within this dynamic range, one is searching for relatively rare low pulse-height events in the presence of a very high singles rate from elastically and inelastically scattered protons, which produce  $\sim 100$  times more light in the liquid scintillator than

do the neutrons of interest. The PSD was performed using a simple electronics scheme, wherein identical copies of the anode signal from each scintillator phototube were fed into two separate charge-integrating ADC's, with separate gates generated by the same constant fraction discriminator. The timing and width of the two gates were chosen so as to integrate only the rising portion of each pulse in one ADC, and only the falling portion in the second, giving pulse heights  $E_1$  and  $E_2$ , respectively. The representative PSD spectrum in Fig. 2 shows the distribution of events with respect to the summed pulse height ( $E_1+E_2$ ) and a pulse shape parameter derived from  $(E_2-E_1)/(E_2+E_1)$ . Good PSD was obtained down to a threshold of 0.4 MeV-ee (equivalent to  $\sim 1.5$  MeV neutron energy).

The energy of the neutron was determined by measuring its time of flight (TOF) between the target and the counter. The 'target signal' was represented by the cyclotron RF signal. Typical ungated (a), PSD-gated gamma (b) and PSD-gated neutron (c) RF-TOF spectra are shown in Fig. 3. The neutron time of flight was calibrated with respect to the location of the prompt  $\gamma$ -peak ( $\gamma$ 's from the target). A software transform was executed (on an event-by-event basis) to deduce from the time of flight of neutrons detected in coincidence with pions the neutron laboratory energy, the neutron energy in the rest frame of the recoiling  $^{13}\text{C}^*$  nucleus, and finally the excitation energy of the daughter  $^{12}\text{C}$  state ( $E_{x12}$ ). The latter two quantities were determined under the assumption of a simple 2-step sequential process:  $p + ^{12}\text{C} \rightarrow \pi^+ + ^{13}\text{C}^*$ ,  $^{13}\text{C}^* \rightarrow n + ^{12}\text{C}^*$ . This transform allowed for direct sorting of the data from individual n-detectors into a single " $^{12}\text{C}$  excitation energy" ( $E_{x12}$ ) spectrum summed over all 7 detectors.



**Figure 2.** Typical pulse-shape discrimination (PSD) spectrum. The separation between  $\gamma$ 's and n's is good down to pulse heights ( $E_1+E_2$ ) equivalent to 0.4 MeV electron-equivalent.

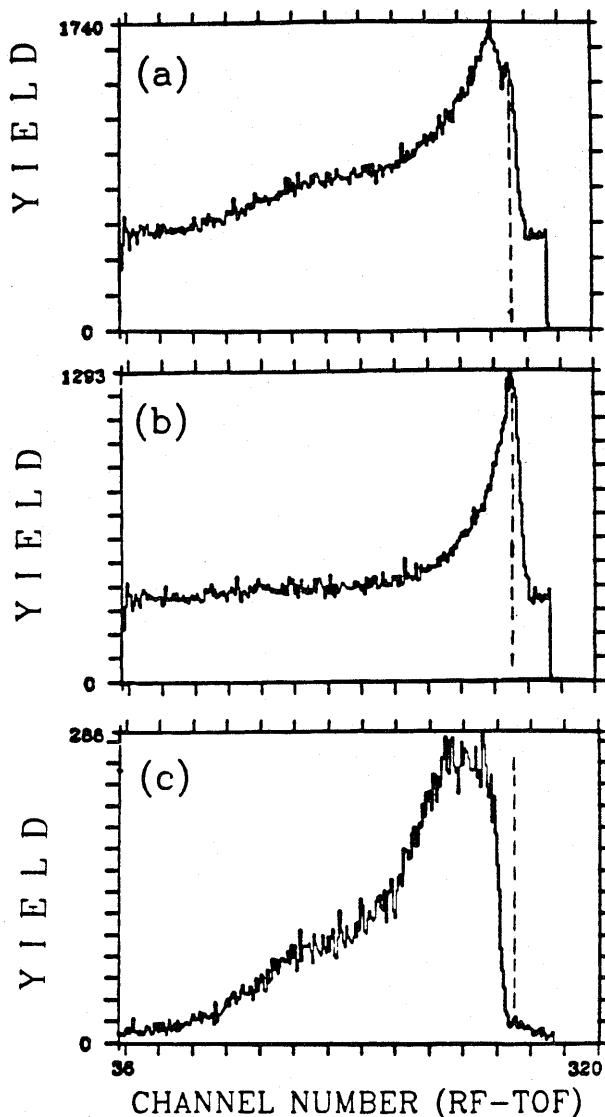


**Figure 3.** Typical n-detector RF-TOF spectra: (a) is the raw spectrum, (b) is the spectrum gated by PSD- $\gamma$ , and (c) is gated by PSD-n. The dotted vertical line indicates the location of the  $\gamma$ -flash from the target. The absence of any feedthrough from this  $\gamma$ -peak in spectrum (c) reflects the good PSD achieved.

The field settings of the QQSP pion spectrometer were chosen so as to position the  $^{12}\text{C}(p,\pi^+)$  21.4-MeV peak in the middle of the focal plane, while detecting within the same momentum bite lower-lying  $^{13}\text{C}$  states down to  $E_x \simeq 6$  MeV. The inclusion of the 6.9 and 7.6-MeV states, with known  $\sim 100\%$  n-decay branching ratios to  $^{12}\text{C}_{g.s.}$ , allow (at least in principle) for built-in calibration of the neutron detection efficiency.  $\pi$ -n TOF information was used to construct a " $\pi$ -n" coincidence time spectrum, spanning about three beam burst periods (each period = 117 ns). The first period provided real as well as accidental  $\pi$ -n (and  $\pi$ - $\gamma$ ) coincidences. The following two were used to monitor the accidental events separately, allowing for later subtraction of accidental coincidences.

Fig. 4 shows the total  $E_{x12}$  real (accidental-subtracted) coincidence spectrum obtained from all 7 neutron detectors for any neutron in coincidence with a  $\pi^+$  corresponding to  $6 \leq E_x(^{13}\text{C}^*) \leq 30$  MeV. This spectrum was acquired over a total effective counting time

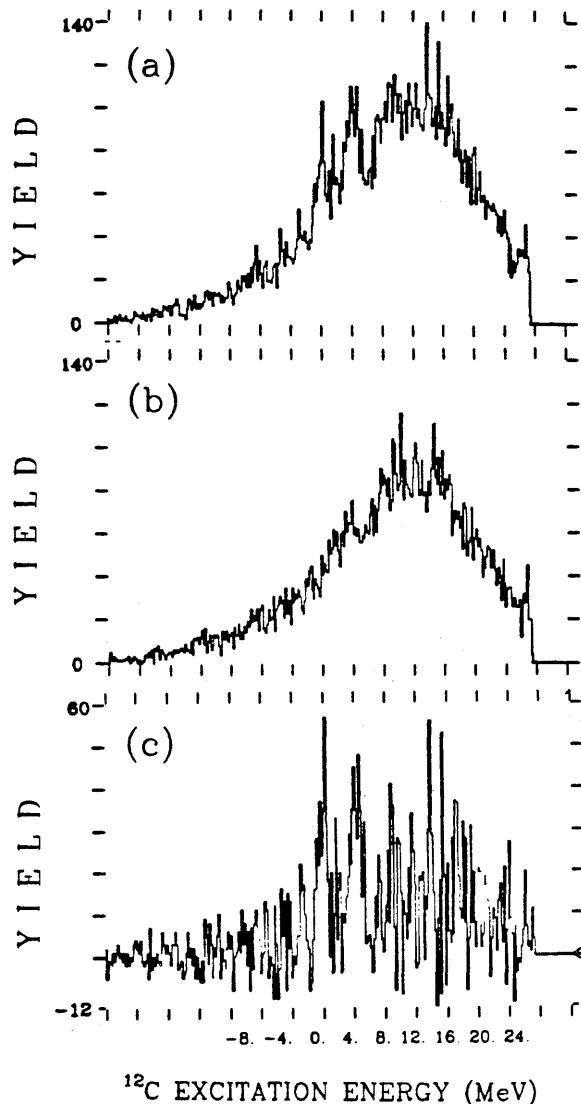


**Figure 4.**  $^{12}\text{C}$  excitation energy spectra summed over all detectors for neutrons in coincidence with pions corresponding to  $6 \leq E_x \leq 30$  MeV in  $^{13}\text{C}$ . Spectrum (a) contains real + accidental coincidences, (b) contains only accidentals, and (c) contains the real coincidences ( $c = a - b$ ). The  $^{12}\text{C}$  daughter states with largest observed decay-neutron yields are the ground and the 4.44-MeV states.

$\sim 45$  hours with an average beam intensity  $\sim 9$  nA, a QQSP solid angle of  $\sim 15$  msr, and a target thickness of  $54.5$  mg/cm $^2$ . In interpreting the spectrum in Fig. 4, one should note that over much of the  $E_x(^{13}\text{C}^*)$  range covered 2-neutron decay is possible; if the  $\pi$ -n coincidence is due to second-chance neutron emission then the value deduced for  $E_{x12}$  will not correspond to a known  $^{12}\text{C}$  state. The largest and clearest neutron yields are observed for the ground ( $0^+$ ) and 4.44-MeV ( $2^+$ ) states in  $^{12}\text{C}$ . Other weaker peaks observed coincide in excitation energy with other known  $^{12}\text{C}$  states, e.g., at 14.1 MeV ( $4^+$ ). (The latter peak appears to be associated mainly with the high- $E_x$  continuum in  $^{12}\text{C}(p,\pi^+)^{13}\text{C}^*$ , and is consistent with the expected preferential population of high-spin states.) "Spurious" peaks are observed, however, at negative excitation energies (e.g.,  $\sim -3$  MeV), and possibly at positive energies not known in the  $^{12}\text{C}$  spectrum. These "peaks" may arise from statistical fluctuations associated with background subtraction and the small number of real coincidence counts. It is conceivable, however, that real

peaks from other neutron decay channels (most likely  $^{12}\text{C}^* \rightarrow ^{11}\text{C}^* + n$ ) also show up in the spectrum. Despite low statistics, the results in Fig. 4 correspond to the first clear observation of  $A(p,\pi N)$  coincidences near threshold.

Fig. 5 shows real (accidental-subtracted)  $E_{x12}$  spectra, gated by the  $^{13}\text{C}$  peaks at 6.86 MeV (a), 7.6 MeV (b), and 9.5 MeV (c). The 6.86-MeV  $(5/2)^+$  state and the  $5/2^+$  and  $3/2^-$  states of the 7.6-MeV complex are each known<sup>7</sup> to decay by neutron emission to the ground state of  $^{12}\text{C}$  with  $\sim 100\%$  absolute branching ratio ( $\Gamma_a$ ). The 9.5-MeV state is known<sup>7</sup> to n-decay to the  $^{12}\text{C}$  4.44-MeV state with  $\Gamma_a \simeq 75\%$ , and to the ground state with  $\Gamma_a \simeq 25\%$ . Indeed, peaks at  $E_x = 0$  MeV in  $^{12}\text{C}$  are observed in spectra (a), (b), and (c). A "4.44-MeV" neutron peak is also probably observed in spectrum (c). However, the decay neutrons leading to this state have laboratory energies  $1.46 \leq T_{lab} \leq 1.63$  (across the angle range covered by the n-detectors), just around the experimental detection threshold ( $\sim 1.5$  MeV), where the detection efficiency is very close (or equal) to zero. A detailed angular

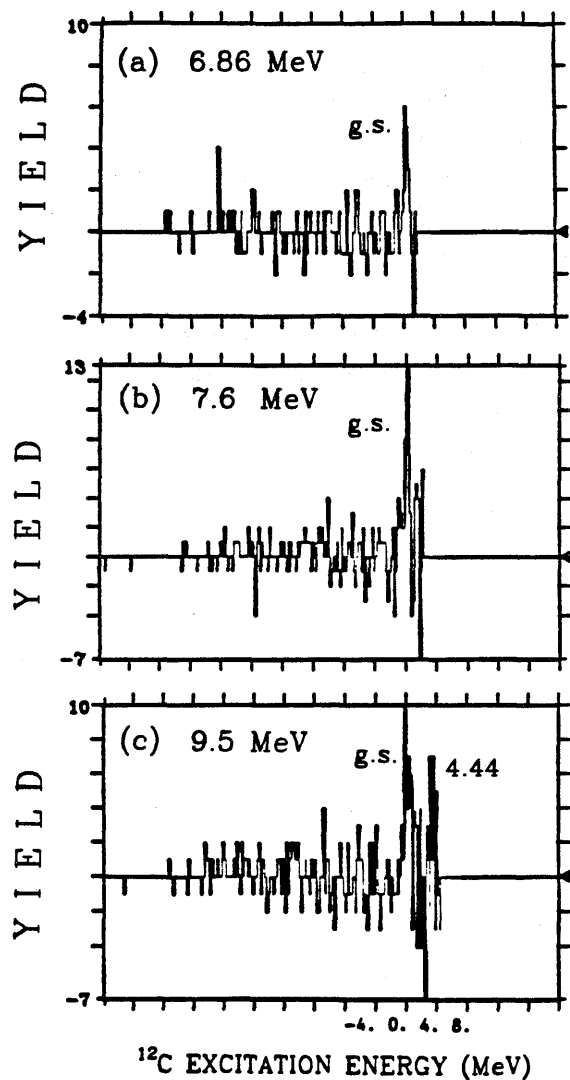


Figure 5.  $^{12}\text{C}$  excitation energy spectra for neutron decays of the  $^{13}\text{C}$  states at (a) 6.86 MeV, (b) 7.6 MeV, and (c) 9.5 MeV.

correlation analysis of the data was not possible, given the extremely low statistics of real-coincidence neutrons detected by any individual detector alone for a given decay channel (typically  $\leq 6$  counts).

The reduction of the final  $E_{x12}$  real-coincidence neutron spectrum for the 21.4-MeV state took into consideration not only the accidental coincidence events, but also the real coincidence events, associated with neutron emission from the continuum. Because of the relatively large width of the 21.4-MeV peak and the large continuum over which it rides, the background was expected to be enhanced compared to the spectra of Fig. 5, which corresponds to narrower pion peaks over much smaller continuum yields. The statistical fluctuations resulting from the combined effects of background subtraction and inadequate running time were therefore severe. Within the large statistical uncertainties, no clear evidence for n-decay of the 21.4-MeV state was observed. Much improved statistics would be needed to draw any firm conclusion regarding the nature of the 21.4-MeV state. Nonetheless, the short production run we took demonstrates the feasibility of the  $\pi^+$ -n coincidence measurement, and indicates the technical concerns important to any future coincidence measurement.

\*Present address: TRIUMF, 4004 Wesbrook Mall, Vancouver, B.C.

1. E. Korkmaz et al., Phys. Rev. Lett. **58**, 104 (1987).
2. S.E. Vigdor, W.W. Jacobs and E. Korkmaz, Phys. Rev. Lett. **58**, 840 (1987).
3. S.M. Aziz et al., Indiana University Scientific and Technical Report-1986, p. 61.
4. S.J. Seestrom-Morris et al., Phys. Rev. C **26**, 954 (1982).
5. J.D. Brown, private communication.
6. See, for example, M.C. Green, Ph.D. Thesis, Indiana University, 1983.
7. F. Ajzenberg-Selove, Nucl. Phys. **A449**, 1 (1986) and references therein.